Tissue-engineered VEGF-impregnated construct to enhance angiogenesis for improved bone regeneration: an in-vivo longitudinal DCE-MRI study

M. Beaumont[1], M. G. DuVal[2], W. A. Farhat[3], G. K. Sàndor[2,4], and H-L. M. Cheng[1,5]

[1]Research Institute & Diagnostic Imaging, The Hospital for Sick Children, Toronto, Ontario, Canada, [2]Oral and Maxillofacial Surgery, University of Toronto, Toronto, Ontario, Canada, [3]Research Institute & Urology, The Hospital for Sick Children, Toronto, Ontario, Canada, [4]Regea Institute for Regenerative Medicine, University of Tampere, Tampere, Finland, [5]Medical Biophysics, University of Toronto, Toronto, Ontario, Canada

INTRODUCTION

Traditional bone reconstruction requires surgery to harvest bone from the patient (usually from the hip, tibia, or scapula), which is associated with limited supply, donor site morbidity, pain, and gait disturbances. Tissue engineering promises to overcome these major drawbacks of autogenous bone grafting. However, establishment of a vascular bed is the greatest obstacle to successful tissue regeneration [1]. The optimal biomaterials and methods for angiogenesis and bone engineering are not well understood. In this in-vivo longitudinal study, we propose a new regeneration paradigm: inserting a biological soft-tissue construct within the bone defect to enhance angiogenesis for improved bone repair. The construct acts as a resorbable scaffold to support desired angiogenesis and cellular activity [2] and as a vector of vascular growth factor (VEGF), known to promote both vessel and bone growth [3]. Dynamic contrast-enhanced MRI (DCE-MRI) is performed to investigate and characterize angiogenesis necessary for bone formation following the proposed paradigm of inserting a VEGF-impregnated tissue-engineered construct within the rabbit calvarial defect.

METHODS

A critical size (non-spontaneous healing) calvarial defect (15mm in diameter) was created surgically in five New Zealand rabbits. The defect was grafted with a tissue-engineered construct fortified with 10ng/g of VEGF. The animals were imaged 1, 2, 3, 6 and 12 weeks after surgery on a 1.5T GE scanner (EXCITE). A rapid 3D T1-mapping method, based on variable flip angles and integrating B1 correction [4], was employed prior to contrast agent (Gd-DTPA) injection to acquire the baseline T1 map (3D FSPGR, TR/TE=8.8/3.4ms, FA=[2 10 20], matrix=256x160x10, FOV=10x10x3cm^3). Dynamic T1-weighted images were acquired using a 3D FSPGR sequence (TR/TE=10.2/3.4ms, FA=60°, matrix=256x128x10, FOV=10x10x3cm^3). After the acquisition of 5 baseline images, Gd-DTPA was administered via the ear vein as a rapid bolus (0.1mmol of Gd / kg) and imaging continued for 6 min post-injection with a time resolution of 8.2s.

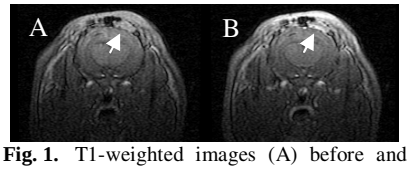

Fig. 1. T1-weighted images (A) before and (B) 60s after Gd-DTPA injection. Imaging time is 3 weeks post-surgery. Arrows indicate the implanted VEGF-impregnated soft-tissue construct.

All analyses were performed on a pixel-wise basis using Matlab (v.7.0). DCE-MRI data were converted into Gd concentration maps using the pre-injection T1 map and the SPGR signal equation. Two regions of interest (ROI) were manually drawn on the construct: the periphery, which corresponds to the early enhancing region, and the centre. For each ROI and for each MR acquisition time point, the Gd concentration median value was calculated. Finally, the area under the median Gd concentration time curve for 60s after contrast agent injection ($IAUC_{60}$) was computed for each ROI and in each rabbit.

RESULTS

Fig.1 shows an example of T1-weighted images (**A**) before and (**B**) 60s after Gd-DTPA injection. Note the presence of two regions in the implanted construct: the highly enhanced periphery and the centre. Fig.2 compares the Gd-DTPA concentration time curves in one rabbit obtained from the two ROIs at four time points (1, 3, 6 and 12 weeks after surgery). The same patterns of contrast agent uptake were observed in all animals. Fig.3 summarizes the $IAUC_{60}$ values measured in all the rabbits for both ROIs throughout the 12 weeks. Both periphery (black bars) and centre (gray bars) regions of the construct show increasing $IAUC_{60}$ values up to 6 weeks, followed by a significant drop at 12 weeks. The only exception occurs at 1 week, where the periphery shows the highest $IAUC_{60}$ level. At this early time point, the periphery enhancement curve (Fig.2, Week 1) exhibits the most rapid initial uptake followed by a distinct washout. Later time points may also show significant enhancement, but the initial uptake is more gradual and washout is not always evident (e.g. Fig.2, Week 6).

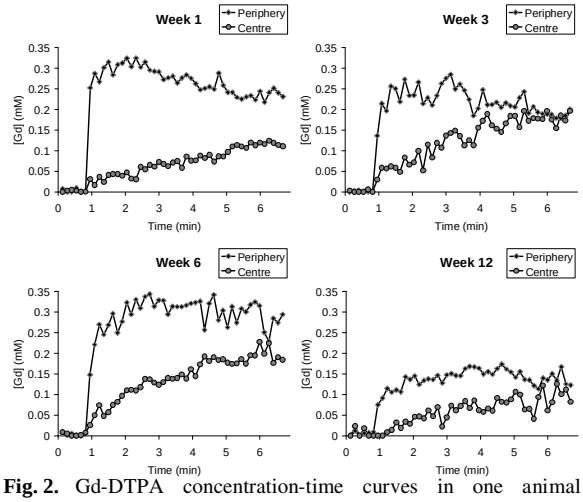

Fig. 2. Gd-DTPA concentration-time curves in one animal between 1 and 12 weeks post-surgery. Periphery and centre of the implanted construct are represented.

DISCUSSION AND CONCLUSIONS

This study shows that DCE-MRI can follow angiogenesis and vasculature establishment in bone formation using the IAUC approach. Furthermore, the regeneration paradigm proposed in this study established vessel development at time points consistent for bony wound repair.

The processes of angiogenesis and bone formation are intimately linked, as stimuli for cell migration and growth require the vasculature as a vehicle. During the first 6 weeks, the $IAUC_{60}$ value increases, corresponding to the expected initiation and establishment of a vessel network in both the periphery and centre of the VEGF-impregnated construct [5]. This new vasculature is necessary for supplying elements to the new bony tissue and initiating calcification and remodeling. Once initiated, these processes decrease their vascular demand, which is consistent with the significant drop of $IAUC_{60}$ values 12 weeks after surgery in the whole construct. In the months following, bone growth and remodeling continue. At 1 week, the high $IAUC_{60}$ observed in the construct periphery due to vessel leakiness (Fig.2 Week 1) is consistent with the natural wound healing process, where both angiogenic and inflammatory responses occurring within the first days following injury [6] are characterized by localized hyper-permeable vessels. Finally, the uptake curves in the core suggest less uptake of contrast agent compared with the periphery and may also reflect diffusion of contrast agent. It remains to be seen if active angiogenesis in the periphery combined with diffusion throughout the core is sufficient for uniform bone regeneration throughout the construct.

Future work will focus on histological studies to further investigate the underlying processes of angiogenesis and mineralization in new bone formation.

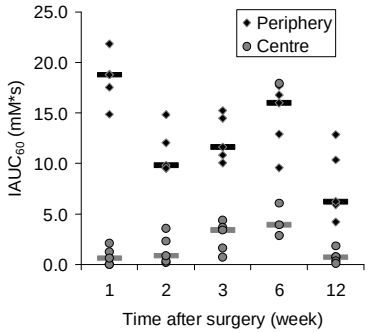

Fig. 3. Evolution of angiogenesis in the periphery and centre of the implanted construct in all animals using the $IAUC_{60}$ metric. Horizontal bars indicate median values.

REFERENCES: [1] Schmedlen et al. Clin Plast Surg 2003; 30:507. [2] Kanczler & Oreffo. Eur Cell Mater 2008; 15:100. [3] Tarkka et al. J Gene Med 2003; 5:560. [4] Cheng &Wright MRM 2006; 55:566. [5] Emad et al. Int J Surg 2006; 4:160. [6] Glowacki. Clin Orthop Rel Res 1998; 355:82.